Stability and optimal measures analysis on the transmission dynamics of Tuberculosis by means of fractional order

Loyinmi, C. Adedapo.

[1]Department of Mathematics, Tai Solarin University of Education, Ijagun. Ogun State.

: loyinmiac@tasued.edu.ng; + (234) 8056751556

Received: 12:05:2026 **Accepted: 02:07:2025** **Published: 07:07:2025**

Abstract:
While being a treatable and preventable disease, tuberculosis (TB) nonetheless poses a serious global health threat and claims millions of lives each year. In this study, a sophisticated mathematical technique from fractional calculus theory is used to explore the complex dynamics of tuberculosis transmission. To capture the subtle progression of tuberculosis infection, the study employs an SEIR model that categorizes the population into distinct compartments. The potential of fractional calculus to transform epidemiological research by simulating the dynamics of infectious diseases was demonstrated through its use. By leveraging the intrinsic flexibility and precision of fractional derivatives, we enhance our understanding of tuberculosis epidemiology and establish the foundation for innovative methods in disease control and prevention. The intricate interactions between susceptible, vaccinated, latent, treated, acute, and recovered individuals in the population were discussed using careful analysis and numerical simulations. The efficiency of several control tactics, including vaccination, treatment of latent and current cases and preventive measures is clarified by key findings from the study. How these interventions affect the dynamics of tuberculosis transmission, community immunity, and disease burden was clarified. In addition, the study provides important information for public health practitioners and policymakers highlighting the varying effectiveness of control methods in reducing transmission and increasing recovery rates. Also, the study is a step forward in epidemiology, providing a comprehensive understanding of the dynamics of TB transmission and the effectiveness of control measures using fractional derivatives. The results of this study are expected to be a guide for evidence-based initiatives, ultimately buttressing international efforts to fight tuberculosis and enhance public health.

Keywords: **Tuberculosis, Fractional calculus, Epidemiology, Transmission dynamics, Control strategies, Mathematical modeling.**

1. Introduction

Mycobacterium tuberculosis is the bacterium that causes tuberculosis (TB) and it mainly affects the lungs but can also affect other organs. The exact place of the infection affects the symptoms, but typical ones include fever, exhaustion, weight loss, chest pain, and a persistent cough. Tuberculosis (TB) is largely an airborne illness. Tiny droplets containing the TB bacterium are released into the air when an infected person coughs, sneezes or speaks. People may then inhale these droplets and get infected with the Tuberculosis (TB) bacteria. The germs might settle in the lungs and begin to develop. They can then travel through the blood to the kidney, spine, and brain, among other areas of the body.

1.3 million Deaths from tuberculosis (TB) were reported in 2022, making it a serious worldwide health concern. Accordingly, it ranks second in terms of infectious causes of death worldwide, after COVID-19 [1–6]. Although TB is preventable and curable, it affects people of all ages and geographical locations. Just a small percentage of those who are afflicted with multidrug-resistant TB (MDR-TB) receive treatment, making it a serious public health concern. However, since 2000, worldwide initiatives have reportedly saved 75 million lives, demonstrating the potential impact of focused interventions. It is predicted that a significant amount of money—roughly US$13 billion per year—will be needed to tame the TB epidemic by 2030, underscoring the urgent need for additional financing and research [4].

The World Health Organization (WHO) plays an important role in leading the international struggle against TB, with an emphasis on innovative researches by developing policy, providing technical assistance, and overseeing progress [7-14]. To scale up TB prevention, diagnosis, treatment, and care, cooperation between nations, partners, and civil society is essential. Establishing standards and norms, encouraging moral behaviour, and strengthening capacity-building programme are top goals. Despite advancements, problems still exist, especially when it comes to tackling the socioeconomic

determinants of TB and TB-HIV co-infection. WHO wants to speed up the process of reaching global TB targets and eventually put an end to the TB epidemic by taking a comprehensive approach and efficiently using resources [4, 6, 15 - 18].

For academics and decision-makers in public health, mathematical modelling has shown to be an essential tool. It has enabled them to better understand the dynamics of disease, create efficient plans for preventing and controlling it, distribute resources effectively, and eventually enhance community health and well-being [8 – 15]. Addressing illnesses like tuberculosis and other global public health issues requires an interdisciplinary approach [8-11, 16, 19 – 27].

Our central aim is to delve into the intricate dynamics, efficacy of control strategies, and computational estimations inherent in the fractional-order TB model under scrutiny. Our inquiry begins by scrutinizing the model's positivity and constraining attributes through conventional mathematical analysis techniques. Following this, we ascertain the fundamental reproduction number utilizing the next-generation matrix approach and assess the model's asymptotic stability. Furthermore, employing an adaptive predictor-corrector algorithm alongside the fourth-order Runge–Kutta (RK4) method, we conduct comprehensive numerical simulations, thereby validating the theoretical insights across a broad spectrum of scenarios. This multifaceted approach ensures a robust examination of the model's behaviour and underpins our understanding through rigorous computational analysis.

2.0 MATERIALS AND METHODS

2.1 Model Description and Formulation

The SEIR model, a mathematical framework with seven compartments, is used to investigate the dynamics of tuberculosis (TB) transmission among human populations. Individuals in the susceptible (S), vaccinated (V), latent (L), treated latent (TL), acute (A), treated acute (TA), and recovered (R) categories make up the entire population, represented by the letter N. Therefore, $N = S + V + L + T_L + A + T_A + R$ is the equation that describes how the population is divided among these compartments.

Every segment outlines a distinct stage in the spread of Tuberculosis over the population. Vulnerable (S) individuals susceptible to the tuberculosis infection, those who have had a tuberculosis vaccination are known as inoculated (V). Dormant (L) are infected individuals who are not exhibiting any symptom at the moment (asymptomatic). Latent people receiving treatment to stop their TB from becoming active are known as treated latent (T_L). People who are actively infected with tuberculosis and have the ability to spread the disease are known as acute (A) patients. Acutely infected people receiving therapy to lessen their contagiousness and encourage healing are known as treated acute (T_A). Recovered (R) are people who are no longer infectious after recovering from a TB illness.

Table 1 provides detailed descriptions of the parameters governing transitions between these compartments within the model, elucidating the dynamics of TB transmission and the impact of interventions such as vaccination and treatment.

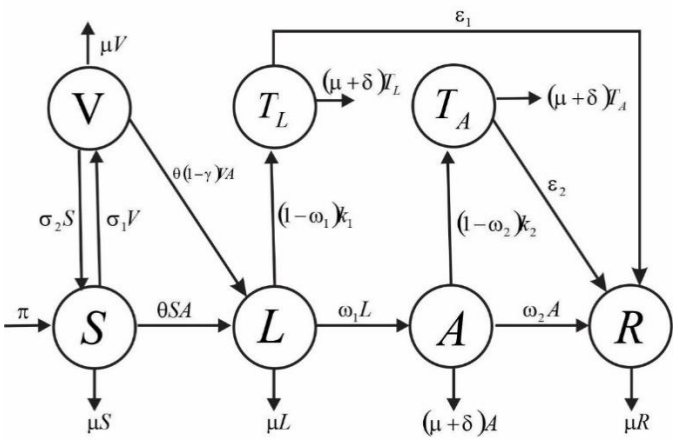

Figure 1: Schematic Diagram of the TB Model

From (Figure 1) and [25-29] the equation governing the Tuberculosis model of Caputo fractional derivatives can be expressed as follows:

$$\left.\begin{aligned}
{}_0^bD_t^\alpha S &= \pi^\alpha + {\sigma_1}^\alpha V - \left(\theta^\alpha A + {\sigma_2}^\alpha + \mu^\alpha\right)S \\
{}_0^bD_t^\alpha V &= {\sigma_2}^\alpha S - \theta^\alpha\left(1-\gamma^\alpha\right)VA - \mu^\alpha V \\
{}_0^bD_t^\alpha L &= \theta^\alpha\left(1-\gamma^\alpha\right)VA + \theta^\alpha SA - \left({\omega_1}^\alpha + \left(1-{\omega_1}^\alpha\right){k_1}^\alpha + \mu^\alpha\right)L \\
{}_0^bD_t^\alpha T_L &= \left(1-{\omega_1}^\alpha\right){k_1}^\alpha L - \left({\varepsilon_1}^\alpha + \mu^\alpha + \delta^\alpha\right)T_L \\
{}_0^bD_t^\alpha A &= {\omega_1}^\alpha L - \left({\omega_2}^\alpha + \left(1-{\omega_2}^\alpha\right){k_2}^\alpha + \mu^\alpha + \delta^\alpha\right)A \\
{}_0^bD_t^\alpha T_A &= \left(1-{\omega_2}^\alpha\right){k_2}^\alpha A - \left({\varepsilon_2}^\alpha + \mu^\alpha + \delta^\alpha\right)T_A \\
{}_0^bD_t^\alpha R &= {\omega_2}^\alpha A + {\varepsilon_1}^\alpha T_L + {\varepsilon_2}^\alpha T_A - \mu^\alpha R
\end{aligned}\right\} \quad (1)$$

Table 1: Variables and Description of the Model

Variables	Description	Values	References
π	Recruitment rate in the susceptible class	1562	Yawuz M. et al,
θ	Rate of infection of susceptible with infected human	0.0005	Yawuz M. et al,
σ_1	Rate of vaccine wanes out	0.1	Oshinubi K. et al,
σ_2	Rate of Vaccination	0.1	Oshinubi K. et al,
γ	Efficacy of the vaccine	0.1	Yawuz M. et al,
ω_1	Transition rate of latent to active	0.00027	Oshinubi K. et al,
ω_2	Recovery rate of Active Individual	0.4	Yawuz M. et al,
k_1	Treatment rate of latent class	0.6	Yawuz M. et al,
k_2	Treatment rate of active individual	0.35	Yawuz M. et al,
δ	Disease induced mortality rate	0.004	Yawuz M. et al,
ε_1	Recovery rate of treated latent	0.5	Yawuz M. et al,
μ	The natural death rate of humans	0.03	Yawuz M. et al,
ε_2	Recovery rate of treated active	0.06	Yawuz M. et al,

Fractional Model Analysis

Positivity of Solution

Given that the fractional model (1) observes the human population, it is imperative to demonstrate that all state variables remain positive throughout $t > 0$.

Theorem 1

Consider the initial
$\{S(0) \geq 0, V(0) \geq 0, L(0) \geq 0, T_L(0) \geq 0, A(0) \geq 0, T_A(0) \geq 0, R(0) \geq 0\} \in D$.

The solution domain $\{S, V, L, T_L, A, T_A, R\}$ of the fractional model exhibits positivity across all parameters within the invariant region $D \subset \Re_+^7$.

Proof

The solution of the model (1) along one state-axis, where other state variables vanish and gives;

$$\left.\begin{aligned}
{}_0^b D_t^\alpha S\,|_{S-axis} &= \pi^\alpha + \sigma_1{}^\alpha V - \left(\theta^\alpha A + \sigma_2{}^\alpha + \mu^\alpha\right)S \\
{}_0^b D_t^\alpha V\,|_{V-axis} &= \sigma_2{}^\alpha S - \theta^\alpha\left(1-\gamma^\alpha\right)VA - \mu^\alpha V \\
{}_0^b D_t^\alpha L\,|_{L-axis} &= \theta^\alpha\left(1-\gamma^\alpha\right)VA + \theta^\alpha SA - \left(\omega_1{}^\alpha + \left(1-\omega_1{}^\alpha\right)k_1{}^\alpha + \mu^\alpha\right)L \\
{}_0^b D_t^\alpha T_L\,|_{T_L-axis} &= \left(1-\omega_1{}^\alpha\right)k_1{}^\alpha L - \left(\varepsilon_1{}^\alpha + \mu^\alpha + \delta^\alpha\right)T_L \\
{}_0^b D_t^\alpha A\,|_{A-axis} &= \omega_1{}^\alpha L - \left(\omega_2{}^\alpha + \left(1-\omega_2{}^\alpha\right)k_2{}^\alpha + \mu^\alpha + \delta^\alpha\right)A \\
{}_0^b D_t^\alpha T_A\,|_{T_A-axis} &= \left(1-\omega_2{}^\alpha\right)k_2{}^\alpha A - \left(\varepsilon_2{}^\alpha + \mu^\alpha + \delta^\alpha\right)T_A \\
{}_0^b D_t^\alpha R\,|_{R-axis} &= \omega_2{}^\alpha A + \varepsilon_1{}^\alpha T_L + \varepsilon_2{}^\alpha T_A - \mu^\alpha R
\end{aligned}\right\} \quad (2)$$

Following the same procedures done for the boundedness of the solution, the solution for the above equations is given as:

$$\left.\begin{aligned}
S(t) &= \frac{\pi^\alpha}{\mu^\alpha} + \left(S(0) - \frac{\pi^\alpha}{\mu^\alpha}\right)E_{\alpha,1}\left(-\mu^\alpha t^\alpha\right) > 0, \\
V(t) &= E(0)E_{\alpha,1}\left(\left(-\theta^\alpha\left(1-\gamma^\alpha\right)A - \mu^\alpha\right)t^\alpha\right) > 0, \\
L(t) &= E(0)E_{\alpha,1}\left(-\left(\omega_1{}^\alpha + \left(1-\omega_1{}^\alpha\right)k_1{}^\alpha + \mu^\alpha\right)t^\alpha\right) > 0, \\
T_L(t) &= E(0)E_{\alpha,1}\left(-\left(\varepsilon_1{}^\alpha + \mu^\alpha + \delta^\alpha\right)t^\alpha\right) > 0, \\
A(t) &= E(0)E_{\alpha,1}\left(-\left(\omega_2{}^\alpha + \left(1-\omega_2{}^\alpha\right)k_2{}^\alpha + \mu^\alpha + \delta^\alpha\right)t^\alpha\right) > 0, \\
T_A(t) &= E(0)E_{\alpha,1}\left(-\left(\varepsilon_2{}^\alpha + \mu^\alpha + \delta^\alpha\right)t^\alpha\right) > 0, \\
R(t) &= E(0)E_{\alpha,1}\left(\left(-\mu^\alpha\right)t^\alpha\right) > 0,
\end{aligned}\right\} \quad (3)$$

The solutions pertaining to the different compartments exhibit non-negativity. In light of the insights derived from Equations (3), it can be deduced that the ensemble remains positively invariant with respect to temporal progression (t).

Also, in the $V - L - T_L - A - T_A - R$ plane, the trajectory solution of the developed fractional model (1) is positive, having $t^* > 0$, such that:

$S(t*) = 0, V(t*) > 0, L(t*) > 0, T_L(t*) > 0, A(t*) > 0, T_A(t*) > 0, R(t*) > 0,$ and $S(t) < S(t^*)$.

On plane

$${}_0^b D_\beta^\alpha S(t)|_{t=t^*} = \pi^\alpha, \quad (4)$$

Now, we apply Caputo fractional derivative mean value theorem, and we have

$$S(t) - S(t*) = \frac{1}{\Gamma(\alpha)}\cdot {}_0^b D_\beta^\alpha(t')(t - t*), t' \in [t*, t) \quad (5)$$

Finally, we have $S(t) > S(t*)$ and this contradicts our assumption earlier for $t^* > 0$. So, the susceptible class $S(t)$ is nonnegative for all time t. Hence, the solution of fractional derivative is positive for all time t.

Boundedness of the Solution

From (1), the total population size is

$N = S + V + L + T_L + A + T_A + R$

And the differential equation involving fractional derivatives for the population is given by:

$D_\beta^\alpha N = {}_0^b D_\beta^\alpha S + {}_0^b D_\beta^\alpha V + {}_0^b D_\beta^\alpha L + {}_0^b D_\beta^\alpha T_L + {}_0^b D_\beta^\alpha A + {}_0^b D_\beta^\alpha T_A + {}_0^b D_\beta^\alpha R$

By incorporating the fractional model system of equations delineating human population dynamics from equation (1) into the preceding expression and meticulously executing the elimination procedure, a profound outcome ensues.

$$D_\beta^\alpha N = \pi^\alpha - \mu^\alpha N - \delta^\alpha(T_L + A + T_A) \quad (6)$$

Theorem 2

The solution of the fractional model (1) is feasible at $t > 0$ if they enter the region $D = \{S, V, L, T_L, A, T_A, R\} \in R^7$.

Proof

Demonstrating the constrained nature of the human population's solution, we revisit equation (3) and employ the Laplace transform on both sides of the equation.

$D_\beta^\alpha N = \pi^\alpha - \mu^\alpha N - \delta^\alpha(T_L + A + T_A)$

at disease free, we have the equation to be

$$D_\beta^\alpha N = \pi^\alpha - \mu^\alpha N \quad (7)$$

Re-arrange the equation above we have,

$$D_\beta^\alpha N + \mu^\alpha N = \pi^\alpha$$

Utilizing the Laplace transformation methodology, we observe

$$L\{D_\beta^\alpha N\}(S) + \mu^\alpha L\{N\}(S) = L\{\pi^\alpha\}(S) \quad (8)$$

The Laplace transform for the Caputo fractional derivate for the above equation is given as [26-27];

$$S^\alpha\psi - \sum_{n=0}^{m-1} S^{\alpha-n-1}N^n(0) + \mu^\alpha\psi = \frac{\pi^\alpha}{S}$$

where $L\{N\}(S) = \psi(S) = \psi$

For $m = 0, 0 < \alpha < 1$, the equation becomes

$$S^\alpha\psi - \sum_{n=0}^{0} S^{\alpha-n-1}N^n(0) + \mu^\alpha\psi = \frac{\pi^\alpha}{S}$$

Now, applying summation property, we have

$$S^\alpha\hat{\lambda} - S^{\alpha-1}N^n(0) + \mu^\alpha\psi = \frac{\pi^\alpha}{S} \quad (9)$$

Then, making $\hat{\lambda}$ the subject of the above equation, we have

$$\psi = \frac{\pi^\alpha S^{-1}}{S^\alpha + \mu^\alpha} + \frac{S^{\alpha-1}}{S^\alpha + \mu^\alpha}N(0) \quad (10)$$

Utilizing the inverse Laplace transformation on both sides of the aforementioned equation yields the following outcome.

$$L^{-1}\{\psi\} = \pi^\alpha L^{-1}\left\{\frac{S^{-1}}{S^\alpha + \mu^\alpha}\right\} + N(0)L^{-1}\left\{\frac{S^{\alpha-1}}{S^\alpha + \mu^\alpha}\right\} \quad (11)$$

Applying the inverse Laplace transform and Mittage-Liffler function [19, 26 -27], we have

$$N(t) = \pi^\alpha\left(t^{\alpha+1-1}E_{\alpha,\alpha+1}\left(-\mu^\alpha t^\alpha\right)\right) + N(0)\left(t^{1-1}E_{\alpha,1}\left(-\mu^\alpha t^\alpha\right)\right) \quad (12)$$

Now, we have

$$N(t)=\pi^{\alpha}t^{\alpha}\left(\frac{1}{-\mu^{\alpha}t^{\alpha}}E_{\alpha,1}\left(-\mu^{\alpha}t^{\alpha}\right)-\frac{1}{-\mu^{\alpha}t^{\alpha}}\sqrt{1}\right)+N(0)E_{\alpha,1}\left(-\mu^{\alpha}t^{\alpha}\right) \quad (13)$$

By simplification, we have

$$N(t)\le\frac{\pi^{\alpha}}{\mu^{\alpha}}+\left(N(0)-\frac{\pi^{\alpha}}{\mu^{\alpha}}\right)E_{\alpha,1}\left(-\mu^{\alpha}t^{\alpha}\right)$$

Finally,

$$\lim_{t\to\infty}N(t)\le\frac{\pi^{\alpha}}{\mu^{\alpha}} \quad (14)$$

Existence and Uniqueness of the Model

Prior to affirming the presence and singular efficacy of the Tuberculosis remedy, it is imperative to initially delineate the core functions as per the fractional derivative model (1), thereby establishing the fundamental basis for our demonstration.

$$\left.\begin{aligned}
\varphi_1&=\pi^{\alpha}+\sigma_1{}^{\alpha}V-\left(\theta^{\alpha}A+\sigma_2{}^{\alpha}+\mu^{\alpha}\right)S\\
\varphi_2&=\sigma_2{}^{\alpha}S-\theta^{\alpha}\left(1-\gamma^{\alpha}\right)VA-\mu^{\alpha}V\\
\varphi_3&=\theta^{\alpha}\left(1-\gamma^{\alpha}\right)VA+\theta^{\alpha}SA-\left(\omega_1{}^{\alpha}+\left(1-\omega_1{}^{\alpha}\right)k_1{}^{\alpha}+\mu^{\alpha}\right)L\\
\varphi_4&=\left(1-\omega_1{}^{\alpha}\right)k_1{}^{\alpha}L-\left(\varepsilon_1{}^{\alpha}+\mu^{\alpha}+\delta^{\alpha}\right)T_L\\
\varphi_5&=\omega_1{}^{\alpha}L-\left(\omega_2{}^{\alpha}+\left(1-\omega_2{}^{\alpha}\right)k_2{}^{\alpha}+\mu^{\alpha}+\delta^{\alpha}\right)A\\
\varphi_6&=\left(1-\omega_2{}^{\alpha}\right)k_2{}^{\alpha}A-\left(\varepsilon_2{}^{\alpha}+\mu^{\alpha}+\delta^{\alpha}\right)T_A\\
\varphi_7&=\omega_2{}^{\alpha}A+\varepsilon_1{}^{\alpha}T_L+\varepsilon_2{}^{\alpha}T_A-\mu^{\alpha}R
\end{aligned}\right\} \quad (15)$$

Also, Let $X(t)=(S,V,L,T_L,A,T_A,R)^T$ and

$U(t,X(t))=(\eta_i)^T, i=1,2,3,4,5,6,7.$

So, we can write the model (1) as follows:

$${}_0^bD_{\beta}^{\alpha}X(t)=\varphi(t,X(t)),X(0)=X_0\ge 0,t\in[0,\zeta],0<\alpha\le 1. \quad (16)$$

In the given expression, condition $K_0\ge 0$ should be considered separately for each component. Problem (16), which is equivalent to model (1), can be defined by integrating the following:

$$X(t)=X_0+\frac{1}{\Gamma(\alpha)}\int_0^{\beta}(\beta-\zeta)^{\alpha-1}\varphi(\zeta,Y(\zeta))d\zeta. \quad (17)$$

Subsequently, we will examine model (1) using the integral representation provided earlier. In this scenario, let $\tau=C([0,\kappa];\Re)$ represent the Banach space comprising all continuous functions that are mapping from the interval $(0,\kappa)$ to $\Re$, equipped with the norm.

$$\|K\|_{\tau}=\sup_{t\in[0,a]}\{|X(t)|\}, \quad (18)$$

and $|K(t)|=|S(t)|+|V(t)|+|L(t)|+|T_L(t)|+|A(t)|+|T_A(t)|+|R(t)|$

Where S,V,L,T_L,A,T_A,R all belong to $C([0,\kappa];\Re)$.

Also, the operator $K:\tau\to\tau$ is defined by

$$(XK)(t)=K_0+\frac{1}{\Gamma(\alpha)}\int_0^{\beta}(\beta-\zeta)^{\alpha-1}\varphi(\zeta,P(\zeta))d\zeta. \quad (19)$$

Therefore, the operator X is properly defined owing to the evident continuity of U.

Theorem 3. Let $\overline{K}=\left(\overline{S},\overline{V},\overline{L},\overline{T_L},\overline{A},\overline{T_A},\overline{R}\right)^T$, the function $\varphi=(\varphi_i)^T$ defined above satisfies

$$\left\|\varphi(t,K(t))-\varphi\left(t,\overline{K}(t)\right)\right\|_{\tau}\le H_k\left\|K-\overline{K}\right\|_{\tau}, \text{ for some } H_k>0.$$

Proof: We have the first component of the kernel φ to be

$$\left|\phi(t,K(t))-\phi\left(t,\overline{K}(t)\right)\right|=\left|\sigma_1{}^{\alpha}\overline{V}-\sigma_1{}^{\alpha}V+\theta^{\alpha}\overline{A}\,\overline{S}-\theta^{\alpha}AS+(\sigma_2{}^{\alpha}+\mu^{\alpha})\overline{S}-(\sigma_2{}^{\alpha}+\mu^{\alpha})S\right| \quad (20)$$

Let $n_1=\max\left\{\overline{S}\,\theta^{\alpha},S\theta^{\alpha}\right\}$ then the equation above can be reduced to

$$\begin{aligned}
&\left|\varphi(t,K(t))-\varphi\left(t,\overline{K}(t)\right)\right|\\
&\le n_1\left|A-\overline{A}\right|+\sigma_1{}^{\alpha}\left|V-\overline{V}\right|+\left(\sigma_2{}^{\alpha}+\mu^{\alpha}\right)\left|S-\overline{S}\right|\\
&\le m_1\left(\left|A-\overline{A}\right|+\left|V-\overline{V}\right|+\left|S-\overline{S}\right|\right),
\end{aligned} \quad (21)$$

Where $m_1=\max\left\{n_1,\sigma_1{}^{\alpha},\sigma_2{}^{\alpha}+\mu^{\alpha}\right\}$.

So,

$$\left|\varphi(t,K(t))-\varphi\left(t,\overline{K}(t)\right)\right|\le m_1\left(\left|A-\overline{A}\right|+\left|V-\overline{V}\right|+\left|S-\overline{S}\right|\right), \quad (22)$$

Similarly, the rest can be demonstrated in a comparable manner. As a result, we can infer that

$$\left\|\varphi(t,K(t))-\varphi\left(t,\overline{K}(t)\right)\right\|\le m_i\left\|P-\overline{P}\right\|, \text{ for}$$

$$m_i=m_1+m_2+m_3+m_4+m_5+m_6+m_7$$

Theorem 4: If the condition $\Theta=\frac{\pi^{\alpha}}{\Gamma(\alpha+1)}$ is satisfied by the preceding theorem, and condition $\Theta m_i<1$ holds, then there exists a sole solution to model (1) on domain $(0,\pi^{\alpha})$ that maintains uniform Lyapunov stability.

Proof: The function $\Theta[0,\pi^{\alpha}]\times\Re_+^7\to\Re_+^7$ is evidently continuous within its specified domain. Consequently, we demonstrate the existence of the solution.

To establish uniqueness, we employ the Banach contraction mapping theorem on the operator X defined earlier. Subsequently, we demonstrate that X functions as both a self-map and a contraction.

By definition, $\sup_{t\in[0,a]}\|\Theta(t,o)\|=\pi^{\alpha}$,

Then, we define $k>\|K_0\|+\Theta\pi^{\alpha}/1-\Theta m_i$ and a close convex set $G_K=\{K\in\tau:\|K\|_{\tau}\le k\}$.

Thus, with regard to the self-mapping attribute, it suffices to demonstrate that $XG_k\subset G_k$. So let $X\in G_k$, then;

$$\|XK\|_\tau = \sup_{t\in[0,\Lambda^\alpha]}\left\{\left|Y_0 + \frac{1}{\Gamma(\alpha)}\int_0^\beta (\beta-\zeta)^{\alpha-1}\Theta(\zeta,K(\zeta))d\zeta\right|\right\} \quad (23)$$

$$\le |K_0| + \frac{1}{\Gamma(\alpha)}\sup_{t\in[0,\Lambda^\alpha]}\left\{\int_0^\beta (\beta-\zeta)^{\alpha-1}\left(|\Theta(\zeta,K(\zeta))-\Theta(\zeta,0)|+|\Theta(\zeta,0)|\right)d\zeta\right\}$$

$$\le |K_0| + \frac{1}{\Gamma(\alpha)}\sup_{t\in[0,\Lambda^\alpha]}\left\{\int_0^\beta (\beta-\zeta)^{\alpha-1}\left(\|\Theta(\zeta,Y(\zeta))-I(\zeta,0)\|_\tau + \|\Theta(\zeta,0)\|\right)d\zeta\right\}$$

$$\le |K_0| + \frac{I_k\|K\|_\tau k+\pi^\alpha}{\Gamma(\alpha)}\sup_{t\in[0,\Lambda^\alpha]}\left\{\int_0^\beta (\beta-\zeta)^{\alpha-1}d\zeta\right\}$$

$$\le |K_0| + \frac{I_k k+\pi^\alpha}{\Gamma(\alpha)}\sup_{t\in[0,\Lambda^\alpha]}\left\{\int_0^\beta (\beta-\zeta)^{\alpha-1}d\zeta\right\}$$

$$= |K_0| + \frac{I_k k+\pi^\alpha}{\Gamma(\alpha+1)}\alpha$$

$$= |K_0| + \Theta\left(I_k k+\pi^\alpha\right) \le k. \quad (24)$$

Consequently, it is observed that operators $XK \subseteq G_k$ and X exhibit characteristics of self-maps within the context. Subsequently, we established the contraction property of operator X. Assuming operators K and $\bar{K}$ conform to the abbreviated dynamical system, the application of the aforementioned theorem result yields the following.

$$\left\|XK - X\bar{K}\right\|_\tau = \sup_{t\in[0,\pi^\alpha]}\left\{\left|(XK)(t)-\left(X\bar{K}\right)(t)\right|\right\} \quad (25)$$

$$= \frac{1}{\Gamma(\alpha)}\sup_{t\in[0,\pi^\alpha]}\left\{\int_0^\beta (\beta-\zeta)^{\alpha-1}\left|\Theta(\zeta,K(\zeta))-\Theta\left(\zeta,\bar{K}(\zeta)\right)\right|d\zeta\right\}$$

$$\le \frac{I_K}{\Gamma(\alpha)}\sup_{t\in[0,\pi^\alpha]}\left\{\int_0^\beta (\beta-\zeta)^{\alpha-1}\left|K(\zeta)-\bar{K}(\zeta)\right|d\zeta\right\}$$

$$\le \Theta I_K\left\|K(\zeta)-\bar{K}(\zeta)\right\|_\alpha \quad (26)$$

Therefore, if $\Theta I_K < 1$ then X acts as a contraction mapping. According to the Banach contraction mapping principle, X possesses a unique fixed point on $[0,\pi^\alpha]$, serving as a solution to model (2). Additionally, the uniform Lyapunov stability of the solutions ensues.

Basic Reproduction Number

We derive the fundamental reproductive rate of model (1) employing the methodology introduced by Diekmann and Heesterbeek, known as the next-generation matrix approach in epidemiological analysis. By applying this technique, $R^f = \rho(GW^{-1})$, the expressions for the novel infection components, denoted as G, and the transition components, denoted as W, within model (1) are deduced.

$$G = \begin{pmatrix} \theta^\alpha\left(1-\gamma^\alpha\right)VA + \theta^\alpha SA \\ 0 \end{pmatrix} \quad (27)$$

$$W = \begin{pmatrix} \left(\omega_1{}^\alpha + \left(1-\omega_1{}^\alpha\right)k_1{}^\alpha + \mu^\alpha\right)L \\ \left(\omega_2{}^\alpha + \left(1-\omega_2{}^\alpha\right)k_2{}^\alpha + \mu^\alpha + \delta^\alpha\right)A \end{pmatrix} \quad (28)$$

Let $E_* = f_{1,}I_A = f_{2,}I_s = f_3$

$$G = \begin{bmatrix} 0 & \theta^\alpha\left(1-\gamma^\alpha\right)V^0 + \theta^\alpha S^0 \\ 0 & 0 \end{bmatrix} \quad (29)$$

Then,

$$W = \begin{bmatrix} \left(\omega_1{}^\alpha + \left(1-\omega_1{}^\alpha\right)k_1{}^\alpha + \mu^\alpha\right) & 0 \\ 0 & \left(\omega_2{}^\alpha + \left(1-\omega_2{}^\alpha\right)k_2{}^\alpha + \mu^\alpha + \delta^\alpha\right) \end{bmatrix} \quad (30)$$

Hence,

$$W^{-1} = \begin{bmatrix} \frac{1}{\left(\omega_1{}^\alpha + \left(1-\omega_1{}^\alpha\right)k_1{}^\alpha + \mu^\alpha\right)} & 0 \\ 0 & \frac{1}{\left(\omega_2{}^\alpha + \left(1-\omega_2{}^\alpha\right)k_2{}^\alpha + \mu^\alpha + \delta^\alpha\right)} \end{bmatrix} \quad (31)$$

The fundamental reproductive rate corresponds to the spectral radius of the matrix representing the propagation of infections to subsequent generations. Thus, from above, we obtain the expression for R^f as

$$R^f = \frac{\theta^\alpha\left(1-\gamma^\alpha\right)V^0 + \theta^\alpha S^0}{\left(\omega_2{}^\alpha + \left(1-\omega_2{}^\alpha\right)k_2{}^\alpha + \mu^\alpha + \delta^\alpha\right)} \quad (32)$$

Analysis of the fractional model

Disease-Free Equilibrium (DFE)

The state of disease absence, $\left(E_D^f\right)$, denoted as the disease-free equilibrium within the fractional model (1), signifies a stable condition wherein the disease undergoes eradication. Through the establishment of steady-state conditions by equating the pertinent variables associated with the disease to zero, model (1) generates the subsequent manifestation for the disease-free equilibrium.

$$E_D^f = \left(\frac{\pi^\alpha}{\mu^\alpha}, 0, 0, 0, 0, 0, 0\right) \quad (33)$$

Now, by setting the state variables associated with the disease to zero and solving, we obtain the following:

$$\left.\begin{aligned} 0 &= \pi^\alpha + \sigma_1{}^\alpha V^0 - \left(\theta^\alpha A^0 + \sigma_2{}^\alpha + \mu^\alpha\right)S^0 \\ 0 &= \sigma_2{}^\alpha S^0 - \theta^\alpha\left(1-\gamma^\alpha\right)V^0A^0 - \mu^\alpha V^0 \\ 0 &= \theta^\alpha\left(1-\gamma^\alpha\right)V^0A^0 + \theta^\alpha S^0A^0 - \left(\omega_1{}^\alpha + \left(1-\omega_1{}^\alpha\right)k_1{}^\alpha + \mu^\alpha\right)L^0 \\ 0 &= \left(1-\omega_1{}^\alpha\right)k_1{}^\alpha L^0 - \left(\varepsilon_1{}^\alpha + \mu^\alpha + \delta^\alpha\right)T_L{}^0 \\ 0 &= \omega_1{}^\alpha L^0 - \left(\omega_2{}^\alpha + \left(1-\omega_2{}^\alpha\right)k_2{}^\alpha + \mu^\alpha + \delta^\alpha\right)A^0 \\ 0 &= \left(1-\omega_2{}^\alpha\right)k_2{}^\alpha A^0 - \left(\varepsilon_2{}^\alpha + \mu^\alpha + \delta^\alpha\right)T_A{}^0 \\ 0 &= \omega_2{}^\alpha A^0 + \varepsilon_1{}^\alpha T_L{}^0 + \varepsilon_2{}^\alpha T_A{}^0 - \mu^\alpha R^0 \end{aligned}\right\} \quad (34)$$

Furthermore, at the point where V, L, T_L, A, T_A and R vanish, we derive:

$$S^0 = \frac{\pi^\alpha}{\mu^\alpha} \quad (35)$$

Therefore, the determination of the equilibrium devoid of disease within the fractional model necessitates the

utilization of basic mathematical computations, as delineated subsequently: $E_D^f = \left(\frac{\pi^\alpha}{\mu^\alpha}, 0,0,0,0,0,0\right)$

Stability Analysis of the DFE

Theorem 4: The state of disease absence within the system $E_D^f = \left(\frac{\pi^\alpha}{\mu^\alpha}, 0,0,0,0,0,0\right)$ exhibits asymptotic stability when all eigenvalues of the Jacobian matrix associated with the system's dynamics are characterized by negativity.

Proof:

In order to substantiate the aforementioned theorem, we undertake the computation of the Jacobian Matrix pertaining to system (1) at the Disease-Free Equilibrium (DFE) point, $E_D^f = \left(\frac{\pi^\alpha}{\mu^\alpha}, 0,0,0,0,0,0\right)$, followed by the assessment of the system's eigenvalues.

The Jacobian Matrix $J(S,V,L,T_L,A,T_A,R)$ of the system at DFE, is given as:

$$J = \begin{bmatrix} -(\sigma_2^\alpha + \mu^\alpha) & \sigma_1^\alpha & 0 & 0 & -\theta^\alpha S^0 & 0 & 0 \\ \sigma_2^\alpha & -\mu^\alpha & 0 & 0 & 0 & 0 & 0 \\ 0 & 0 & -(\omega_1^\alpha + (1-\omega_1^\alpha)k_1^\alpha + \mu^\alpha) & 0 & \theta^\alpha S^0 & 0 & 0 \\ 0 & 0 & (1-\omega_1^\alpha)k_1^\alpha & -(\varepsilon_1^\alpha + \mu^\alpha + \delta^\alpha) & 0 & 0 & 0 \\ 0 & 0 & \omega_1^\alpha & 0 & -(\omega_2^\alpha + (1-\omega_2^\alpha)k_2^\alpha + \mu^\alpha + \delta^\alpha) & 0 & 0 \\ 0 & 0 & 0 & (1-\omega_2^\alpha)k_2^\alpha & 0 & -(\varepsilon_2^\alpha + \mu^\alpha + \delta^\alpha) & 0 \\ 0 & 0 & 0 & \varepsilon_1^\alpha & \omega_2^\alpha & \varepsilon_2^\alpha & -\mu^\alpha \end{bmatrix}$$

$$|J-\lambda| = \begin{bmatrix} -(\sigma_2^\alpha + \mu^\alpha) - \lambda & \sigma_1^\alpha & 0 & 0 & -\theta^\alpha S^0 & 0 & 0 \\ \sigma_2^\alpha & -\mu^\alpha - \lambda & 0 & 0 & 0 & 0 & 0 \\ 0 & 0 & -(\omega_1^\alpha + (1-\omega_1^\alpha)k_1^\alpha + \mu^\alpha) - \lambda & 0 & \theta^\alpha S^0 & 0 & 0 \\ 0 & 0 & (1-\omega_1^\alpha)k_1^\alpha & -(\varepsilon_1^\alpha + \mu^\alpha + \delta^\alpha) - \lambda & 0 & 0 & 0 \\ 0 & 0 & \omega_1^\alpha & 0 & -(\omega_2^\alpha + (1-\omega_2^\alpha)k_2^\alpha + \mu^\alpha + \delta^\alpha) - \lambda & 0 & 0 \\ 0 & 0 & 0 & (1-\omega_2^\alpha)k_2^\alpha & 0 & -(\varepsilon_2^\alpha + \mu^\alpha + \delta^\alpha) - \lambda & 0 \\ 0 & 0 & 0 & \varepsilon_1^\alpha & \omega_2^\alpha & \varepsilon_2^\alpha & -\mu^\alpha - \lambda \end{bmatrix}$$

In the last column $-\mu^\alpha - \lambda$ is the only non-null entry

Hence $\lambda_1 = -\mu^\alpha < 0$

By deleting the last row and columns of the above matrix, we have a new matrix:

$$J_1 = \begin{bmatrix} -(\sigma_2^\alpha + \mu^\alpha) - \lambda & \sigma_1^\alpha & 0 & 0 & -\theta^\alpha S^0 & 0 \\ \sigma_2^\alpha & -\mu^\alpha - \lambda & 0 & 0 & 0 & 0 \\ 0 & 0 & -(\omega_1^\alpha + (1-\omega_1^\alpha)k_1^\alpha + \mu^\alpha) - \lambda & 0 & \theta^\alpha S^0 & 0 \\ 0 & 0 & (1-\omega_1^\alpha)k_1^\alpha & -(\varepsilon_1^\alpha + \mu^\alpha + \delta^\alpha) - \lambda & 0 & 0 \\ 0 & 0 & \omega_1^\alpha & 0 & -(\omega_2^\alpha + (1-\omega_2^\alpha)k_2^\alpha + \mu^\alpha + \delta^\alpha) - \lambda & 0 \\ 0 & 0 & 0 & (1-\omega_2^\alpha)k_2^\alpha & 0 & -(\varepsilon_2^\alpha + \mu^\alpha + \delta^\alpha) - \lambda \end{bmatrix}$$

$-(\varepsilon_2^\alpha + \mu^\alpha + \delta^\alpha) - \lambda$ is also the only non-zero entry in the last column:

Hence $\lambda_2 = -(\varepsilon_2^\alpha + \mu^\alpha + \delta^\alpha) < 0$

Similarly, by deleting the last row and columns of the matrix above, we have a new matrix:

$$J_2 = \begin{bmatrix} -(\sigma_2^\alpha + \mu^\alpha) - \lambda & \sigma_1^\alpha & 0 & 0 & -\theta^\alpha S^0 \\ \sigma_2^\alpha & -\mu^\alpha - \lambda & 0 & 0 & 0 \\ 0 & 0 & -(\omega_1^\alpha + (1-\omega_1^\alpha)k_1^\alpha + \mu^\alpha) - \lambda & 0 & \theta^\alpha S^0 \\ 0 & 0 & (1-\omega_1^\alpha)k_1^\alpha & -(\varepsilon_1^\alpha + \mu^\alpha + \delta^\alpha) - \lambda & 0 \\ 0 & 0 & \omega_1^\alpha & 0 & -(\omega_2^\alpha + (1-\omega_2^\alpha)k_2^\alpha + \mu^\alpha + \delta^\alpha) - \lambda \end{bmatrix}$$

Similarly, in the third column $-(\varepsilon_1^\alpha + \mu^\alpha + \delta^\alpha) - \lambda$ is the only non-null entry:

Hence $\lambda_3 = -(\varepsilon_1^\alpha + \mu^\alpha + \delta^\alpha) < 0$

Continual reduction of preceding matrix to its echelon form gives:

$$J_2 = \begin{bmatrix} -(\sigma_2^\alpha + \mu^\alpha) - \lambda & \sigma_1^\alpha & 0 & -\theta^\alpha S^0 \\ \sigma_2^\alpha & -\mu^\alpha - \lambda & 0 & 0 \\ 0 & 0 & -(\omega_1^\alpha + (1-\omega_1^\alpha)k_1^\alpha + \mu^\alpha) - \lambda & \theta^\alpha S^0 \\ 0 & 0 & \omega_1^\alpha & -(\omega_2^\alpha + (1-\omega_2^\alpha)k_2^\alpha + \mu^\alpha + \delta^\alpha) - \lambda \end{bmatrix}$$

Clearly, the remaining eigenvalues which can be deduce from matrix J_2 are represented by the diagonal elements in the matrix shown above. It is evident that these eigenvalues are purely real and do not contain any complex components. The signs of these eigenvalues are of utmost importance in determining the stability of the DFE. In this particular circumstance, it is observed that all eigenvalues exhibit negative real components, thereby affirming the local asymptotic stability of the Model.

Behaviour of the Model in Global Sense

Theorem 5

The globally asymptotically stable status of the non-negative equilibrium point of model (1) is established, given certain conditions, $H^0 > 1$.

Proof

To ascertain the worldwide steadiness of this equilibrium E_D^f, we formulate the ensuing Lyapunov function utilizing the approach delineated in the referenced study [10].

$$\begin{aligned} H(S,V,L,T_L,A,T_A,R) = {} & \left(S - S^0 - S^0 \log\frac{S^0}{S}\right) + \left(V - V^0 - V^0 \log\frac{V^0}{V}\right) + \left(L - L^0 - L^0 \log\frac{L^0}{L}\right) \\ & + \left(T_L - T_L^0 - T_L^0 \log\frac{T_L^0}{T_L}\right) + \left(A - A^0 - A^0 \log\frac{A^0}{A}\right) \\ & + \left(T_A - T_A^0 - T_A^0 \log\frac{T_A^0}{T_A}\right) + \left(R - R^0 - R^0 \log\frac{R^0}{R}\right) \end{aligned} \tag{36}$$

The gradient of H along the trajectory of the solution as delineated in equation (1) through explicit computational methods.

$$\begin{aligned} \frac{dH}{dt} = {} & \left(\frac{S-S^0}{S}\right)\frac{dS_H}{dt} + \left(\frac{V-V^0}{V}\right)\frac{dV}{dt} + \left(\frac{L-L^0}{L}\right)\frac{dL}{dt} \\ & + \left(\frac{T_L - T_L^0}{T_L}\right)\frac{dT_L}{dt} + \left(\frac{A-A^0}{A}\right)\frac{dA}{dt} + \left(\frac{T_A - T_A^0}{T_A}\right)\frac{dT_A}{dt} + \left(\frac{R-R^0}{R}\right)\frac{dR}{dt} \end{aligned} \tag{37}$$

In furtherance of the aforementioned equation, we extend our analysis to segregate the positive and negative components, denoted as Q and O respectively.

$$\frac{dH}{dt} = Q - O \tag{38}$$

$$\begin{aligned} Q = {} & \left(1 - \frac{S^0}{S}\right)(\pi^\alpha + \sigma_1^\alpha V) + \left(1 - \frac{V^0}{V}\right)\sigma_2^\alpha S + \left(1 - \frac{L^0}{L}\right)(\theta^\alpha(1-\gamma^\alpha)VA + \theta^\alpha SA) \\ & + \left(1 - \frac{T_L^0}{T_L}\right)(1-\omega_1^\alpha)k_1^\alpha L + \left(1 - \frac{A^0}{A}\right)\omega_1^\alpha L + \left(1 - \frac{T_A^0}{T_A}\right)(1-\omega_2^\alpha)k_2^\alpha A + \left(1 - \frac{R^0}{R}\right)(\omega_2^\alpha A + \varepsilon_1^\alpha T_L + \varepsilon_2^\alpha T_A) \end{aligned}$$

Similarly,

$$\begin{aligned} O = {} & \frac{(S-S^0)^2}{S}(\theta^\alpha A + \sigma_2^\alpha + \mu^\alpha) + \frac{(V-V^0)^2}{V}(\theta^\alpha(1-\gamma^\alpha)A + \mu^\alpha) \\ & + \frac{(L-L^0)^2}{L}(\omega_1^\alpha + (1-\omega_1^\alpha)k_1^\alpha + \mu^\alpha) + \frac{(T_L - T_L^0)^2}{T_L}(\varepsilon_1^\alpha + \mu^\alpha + \delta^\alpha) \\ & + \frac{(A-A^0)^2}{A}(\omega_2^\alpha + (1-\omega_2^\alpha)k_2^\alpha + \mu^\alpha + \delta^\alpha) \\ & + \frac{(T_A - T_A^0)^2}{T_A}(\varepsilon_2^\alpha + \mu^\alpha + \delta^\alpha) + \frac{(R-R^0)^2}{R}\mu^\alpha \end{aligned} \tag{39}$$

If condition $Q < O$, it will result in negative definiteness of $\frac{dH}{dt}$ along the trajectory of the system. Consequently, it suggests that only at the disease-free equilibrium (E_0) will $\frac{dH}{dt} \le 0$. This observation implies the global stability of the system at the disease-free equilibrium.

Infection Persistence Equilibrium

Theorem 6.

The fractional model system (1) has a unique endemic equilibrium $e_1 = \left(S^*, V^*, L^*, T_L{}^*, A^*, T_A{}^*, R^*\right)$.

At equilibrium point, equation (1) are written as;

$$\left.\begin{aligned}
0 &= \pi^\alpha + \sigma_1{}^\alpha V^* - \left(\theta^\alpha A^* + \sigma_2{}^\alpha + \mu^\alpha\right)S^* \\
0 &= \sigma_2{}^\alpha S^* - \theta^\alpha\left(1-\gamma^\alpha\right)V^*A^* - \mu^\alpha V^* \\
0 &= \theta^\alpha\left(1-\gamma^\alpha\right)V^*A^* + \theta^\alpha S^*A^* - \left(\omega_1{}^\alpha + \left(1-\omega_1{}^\alpha\right)k_1{}^\alpha + \mu^\alpha\right)L^* \\
0 &= \left(1-\omega_1{}^\alpha\right)k_1{}^\alpha L^* - \left(\varepsilon_1{}^\alpha + \mu^\alpha + \delta^\alpha\right)T_L{}^* \\
0 &= \omega_1{}^\alpha L^* - \left(\omega_2{}^\alpha + \left(1-\omega_2{}^\alpha\right)k_2{}^\alpha + \mu^\alpha + \delta^\alpha\right)A^* \\
0 &= \left(1-\omega_2{}^\alpha\right)k_2{}^\alpha A^* - \left(\varepsilon_2{}^\alpha + \mu^\alpha + \delta^\alpha\right)T_A{}^* \\
0 &= \omega_2{}^\alpha A^* + \varepsilon_1{}^\alpha T_L{}^* + \varepsilon_2{}^\alpha T_A{}^* - \mu^\alpha R^*
\end{aligned}\right\} \quad (40)$$

Furthermore, leveraging a numerical simulation technique, we acquire the endemic equilibrium as a result of a specific problem-solving approach**.**

Fractional Optimal Control Strategies

Here are pivotal elements of fractional optimal control for tuberculosis (TB): we alleviate the transmission rate through c_1, where c_1 symbolizes individual vaccination, c_2 denotes the effort of treatment on latent individuals, and c_3 represents the effort of treatment of active individuals. Based on these premises, the ensuing collection of novel Caputo fractional derivatives equations is formulated:

$$\left.\begin{aligned}
{}_0^bD_t^\alpha S &= \pi^\alpha + \sigma_1{}^\alpha V - \left(\theta^\alpha A + c_1{}^\alpha + \mu^\alpha\right)S \\
{}_0^bD_t^\alpha V &= c_1{}^\alpha S - \theta^\alpha\left(1-\gamma^\alpha\right)VA - \mu^\alpha V \\
{}_0^bD_t^\alpha L &= \theta^\alpha\left(1-\gamma^\alpha\right)VA + \theta^\alpha SA - \left(\omega_1{}^\alpha + \left(1-\omega_1{}^\alpha\right)c_2{}^\alpha + \mu^\alpha\right)L \\
{}_0^bD_t^\alpha T_L &= \left(1-\omega_1{}^\alpha\right)c_2{}^\alpha L - \left(\varepsilon_1{}^\alpha + \mu^\alpha + \delta^\alpha\right)T_L \\
{}_0^bD_t^\alpha A &= \omega_1{}^\alpha L - \left(\omega_2{}^\alpha + \left(1-\omega_2{}^\alpha\right)c_3{}^\alpha + \mu^\alpha + \delta^\alpha\right)A \\
{}_0^bD_t^\alpha T_A &= \left(1-\omega_2{}^\alpha\right)c_3{}^\alpha A - \left(\varepsilon_2{}^\alpha + \mu^\alpha + \delta^\alpha\right)T_A \\
{}_0^bD_t^\alpha R &= \omega_2{}^\alpha A + \varepsilon_1{}^\alpha T_L + \varepsilon_2{}^\alpha T_A - \mu^\alpha R
\end{aligned}\right\} \quad (41)$$

Analysis of the Model Integrating Preventive Interventions

In this section, a framework has been developed to integrate a precise functional, emphasizing its controllability via the implementation of Pontryagin's Maximum Principle. Focusing on the fractional optimal setup outlined in equation system (41), emphasis has been placed on a significant control challenge, elucidated prior to engaging in thorough global optimization. The intricate task of selecting the most effective strategies is encapsulated by the functional objective denoted as H. The overarching predetermined objective involves diminishing the population across all categories, all within a specified timeframe [0, T].

Let $M = \{(c_1, c_2, c_3) \in M\}$ be Lebesgue measurable on $[0,1]$,

Where $0 \le c_j(t) \le 1 \in [0,1], j = 1,2,3$ (42)

Next, we introduce the target function, G, to be

$$G(c_1, c_2, c_3) = \int_0^T \left(X_1T_A + X_2T_L + X_3V + \frac{1}{2}\left(Y_1c_1^2 + Y_2c_2^2 + Y_3c_3^2\right)\right)dt \quad (43)$$

constraint to

$$\left.\begin{aligned}
{}_0^bD_t^\alpha S &= \pi^\alpha + \sigma_1{}^\alpha V - \left(\theta^\alpha A + c_1{}^\alpha + \mu^\alpha\right)S \\
{}_0^bD_t^\alpha V &= c_1{}^\alpha S - \theta^\alpha\left(1-\gamma^\alpha\right)VA - \mu^\alpha V \\
{}_0^bD_t^\alpha L &= \theta^\alpha\left(1-\gamma^\alpha\right)VA + \theta^\alpha SA - \left(\omega_1{}^\alpha + \left(1-\omega_1{}^\alpha\right)c_2{}^\alpha + \mu^\alpha\right)L \\
{}_0^bD_t^\alpha T_L &= \left(1-\omega_1{}^\alpha\right)c_2{}^\alpha L - \left(\varepsilon_1{}^\alpha + \mu^\alpha + \delta^\alpha\right)T_L \\
{}_0^bD_t^\alpha A &= \omega_1{}^\alpha L - \left(\omega_2{}^\alpha + \left(1-\omega_2{}^\alpha\right)c_3{}^\alpha + \mu^\alpha + \delta^\alpha\right)A \\
{}_0^bD_t^\alpha T_A &= \left(1-\omega_2{}^\alpha\right)c_3{}^\alpha A - \left(\varepsilon_2{}^\alpha + \mu^\alpha + \delta^\alpha\right)T_A \\
{}_0^bD_t^\alpha R &= \omega_2{}^\alpha A + \varepsilon_1{}^\alpha T_L + \varepsilon_2{}^\alpha T_A - \mu^\alpha R
\end{aligned}\right\} \quad (44)$$

The concluding time point is denoted by the parameter T with coefficients aligning with the weight constants attributed to the virus across distinct groups. The focal point in this segment is the reduction of operational costs, as outlined in equation (48). Additionally, our exploration extends to include an examination of the social expenses $Y_1c_1^2, Y_2c_2^2,$ and $Y_3c_3^2$ linked to the described scenario.

To achieve the goal of tackling the control issue, our effort is focused on pinpointing $\left(c_1^*(t), c_2^*(t), c_3^*(t)\right)$, the functionalities in order to

$$G\left(c_1^*(t), c_2^*(t), c_3^*(t)\right) = \min\{G(c), (c) \in M\} \quad (45)$$

Existence of an Optimal Control Solution

Theorem: Considering equation (45), let $G(c)$ be the optimal control subject to (49), with the initial condition at t=0. The optimal control is given by: $\left(c_1^*(t), c_2^*(t), c_3^*(t)\right)$, such that

$$G\left(c_1^*(t), c_2^*(t), c_3^*(t)\right) = \min\{G(c), (c) \in M\}$$

Proof: The convex nature of the integrand regarding the control measures G ensures the presence of an optimal solution for control.

Following this, it is crucial to delineate the most effective resolution. The Lagrangian is articulated in the subsequent manner:

$$M_G = X_1T_A + X_2T_L + X_3V + \frac{1}{2}\left(Y_1c_1^2 + Y_2c_2^2 + Y_3c_3^2\right)t \quad (46)$$

The Hamiltonian function is given as;

$$\begin{aligned}
H_G &= X_1T_A + X_2T_L + X_3V + \frac{1}{2}\left(Y_1c_1^2 + Y_2c_2^2 + Y_3c_3^2\right)t \\
&+ \Lambda_S\left[S^{'}\right] + \Lambda_V\left[V^{'}\right] + \Lambda_L\left[L^{'}\right] + \Lambda_{T_L}\left[T_L^{'}\right] + \Lambda_A\left[A^{'}\right] + \Lambda_{T_A}\left[T_A^{'}\right] + \Lambda_R\left[R^{'}\right]
\end{aligned} \quad (47)$$

and

$$\left.\begin{aligned}
{}_0^bD_t^\alpha S &= \pi^\alpha + \sigma_1{}^\alpha V - \left(\theta^\alpha A + c_1{}^\alpha + \mu^\alpha\right)S \\
{}_0^bD_t^\alpha V &= c_1{}^\alpha S - \theta^\alpha\left(1-\gamma^\alpha\right)VA - \mu^\alpha V \\
{}_0^bD_t^\alpha L &= \theta^\alpha\left(1-\gamma^\alpha\right)VA + \theta^\alpha SA - \left(\omega_1{}^\alpha + \left(1-\omega_1{}^\alpha\right)c_2{}^\alpha + \mu^\alpha\right)L \\
{}_0^bD_t^\alpha T_L &= \left(1-\omega_1{}^\alpha\right)c_2{}^\alpha L - \left(\varepsilon_1{}^\alpha + \mu^\alpha + \delta^\alpha\right)T_L \\
{}_0^bD_t^\alpha A &= \omega_1{}^\alpha L - \left(\omega_2{}^\alpha + \left(1-\omega_2{}^\alpha\right)c_3{}^\alpha + \mu^\alpha + \delta^\alpha\right)A \\
{}_0^bD_t^\alpha T_A &= \left(1-\omega_2{}^\alpha\right)c_3{}^\alpha A - \left(\varepsilon_2{}^\alpha + \mu^\alpha + \delta^\alpha\right)T_A \\
{}_0^bD_t^\alpha R &= \omega_2{}^\alpha A + \varepsilon_1{}^\alpha T_L + \varepsilon_2{}^\alpha T_A - \mu^\alpha R
\end{aligned}\right\} \quad (48)$$

Provided $\Lambda_j, j \in \{S,V,L,T_L,A,T_A,R\}$ are discrete and mutually exclusive variables.

We are ready to apply the fundamental prerequisites to the Hamiltonian (H_G) for examination. To uncover the adjunct equation and satisfy the transversality condition, we utilize the Hamiltonian. Through the application of differential processes, we ascertain the values linked to the variables S,V,L,T_L,A,T_A,R concerning the Hamiltonian. This culminates in the derivation of the adjunct equation, articulated as follows:

$${}_0^bD_{t_f}^\alpha S = -\frac{\partial H_G}{dS} = \left[\left(\theta^\alpha A + c_1{}^\alpha + \mu^\alpha\right)\Lambda_S - c_1{}^\alpha\Lambda_V - \theta^\alpha A\Lambda_L\right]$$

$${}_0^bD_{t_f}^\alpha V = -\frac{\partial H_G}{dV} = \left[-X_3 - \sigma_1{}^\alpha\Lambda_S + \left(\theta^\alpha\left(1-\gamma^\alpha\right)A + \mu^\alpha\right)\Lambda_V - \theta^\alpha\left(1-\gamma^\alpha\right)A\Lambda_L\right]$$

$${}_0^bD_{t_f}^\alpha L = -\frac{\partial H_G}{dL} = \left[\left(\omega_1{}^\alpha + \left(1-\omega_1{}^\alpha\right)c_2{}^\alpha + \mu^\alpha\right)\Lambda_L - \left(1-\omega_1{}^\alpha\right)c_2{}^\alpha\Lambda_{T_L} - \omega_1{}^\alpha\Lambda_A\right]$$

$${}_0^bD_{t_f}^\alpha T_L = -\frac{\partial H_G}{dT_L} = \left[-X_2 + \left(\varepsilon_1{}^\alpha + \mu^\alpha + \delta^\alpha\right)\Lambda_{T_L} - \varepsilon_1{}^\alpha\Lambda_R\right] \quad (49)$$

$${}_0^bD_{t_f}^\alpha A = -\frac{\partial H_G}{dA} = \begin{bmatrix} \theta^\alpha S\Lambda_S + \theta^\alpha\left(1-\gamma^\alpha\right)V\Lambda_V - \left(\theta^\alpha\left(1-\gamma^\alpha\right)V + \theta^\alpha S\right)\Lambda_L \\ + \left(\omega_2{}^\alpha + \left(1-\omega_2{}^\alpha\right)c_3{}^\alpha + \mu^\alpha + \delta^\alpha\right)\Lambda_A \\ - \left(1-\omega_2{}^\alpha\right)c_3{}^\alpha\Lambda_{T_A} - \omega_2{}^\alpha\Lambda_R \end{bmatrix}$$

$${}_0^bD_{t_f}^\alpha T_A = -\frac{\partial H_G}{dT_A} = \left[-X_1 + \left(\varepsilon_2{}^\alpha + \mu^\alpha + \delta^\alpha\right)\Lambda_{T_A} - \varepsilon_2{}^\alpha\Lambda_R\right]$$

$${}_0^bD_{t_f}^\alpha R = -\frac{\partial H_G}{dR} = \mu^\alpha\Lambda_R$$

Given the transversality conditions, we have $\Lambda_j, j \in \{S,V,L,T_L,A,T_A,R\}$.

In the effort to minimize the Hamiltonian, represented as H_G, concerning the optimal control variables, we commence the differentiation process in relation to $c = c_1, c_2, c_3$. This process yields a series of mathematical expressions, subsequently equated to zero to ascertain the optimal configuration of controls. This approach ultimately leads to the derivation of the desired optimal control solution.

Taking (47), thus we have

$$\begin{aligned}
\frac{dH_G}{dc_1} &= Y_1c_1 - S\Lambda_S + S\Lambda_V, \\
\frac{dH_G}{dc_2} &= Y_2c_2 - \left(1-\omega_1{}^\alpha\right)L\Lambda_L + \left(1-\omega_1{}^\alpha\right)L\Lambda_{T_L} \\
\frac{dH_G}{dc_3} &= Y_3c_3 - \left(1-\omega_2{}^\alpha\right)A\Lambda_A + \left(1-\omega_2{}^\alpha\right)A\Lambda_{T_A}
\end{aligned} \quad (50)$$

We proceed with the process of obtaining the optimal control solution:

$$\begin{aligned}
c_1{}^* &= \frac{S\left(\Lambda_S - \Lambda_V\right)}{Y_1}, \quad c_2{}^* = \frac{\left(1-\omega_1{}^\alpha\right)L\left(\Lambda_L - \Lambda_{T_L}\right)}{Y_2}, \\
c_3{}^* &= \frac{\left(1-\omega_2{}^\alpha\right)A\left(\Lambda_A - \Lambda_{T_A}\right)}{Y_3}
\end{aligned} \quad (51)$$

Incorporating the boundary parameters, the solution is articulated as follows:

$$c_1 *= min\{1, max\{0, U_1\}\};$$

$$c_2 *= min\{1, max\{0, U_2\}\};$$

$$c_3 *= min\{1, max\{0, U_3\}\},$$

with

$$U_1 = \frac{S\left(\Lambda_S - \Lambda_V\right)}{Y_1}, \quad U_2 = \frac{\left(1-\omega_1{}^\alpha\right)L\left(\Lambda_L - \Lambda_{T_L}\right)}{Y_2},$$

$$U_3 = \frac{\left(1-\omega_2{}^\alpha\right)A\left(\Lambda_A - \Lambda_{T_A}\right)}{Y_3} \quad \text{Proved}$$

Numerical Simulation

This segment presents illustrative numerical simulations aimed at elucidating the dynamics inherent in the Caputo fractional-order deterministic nonlinear mathematical model for tuberculosis (TB). The simulations were conducted utilizing MATLAB software, employing parameter values delineated in Tables 1 and 2.

Table 2: Compartment values

Compartment	Value
S	600
V	100
L	400
T_L	200
A	110
T_A	100
R	30

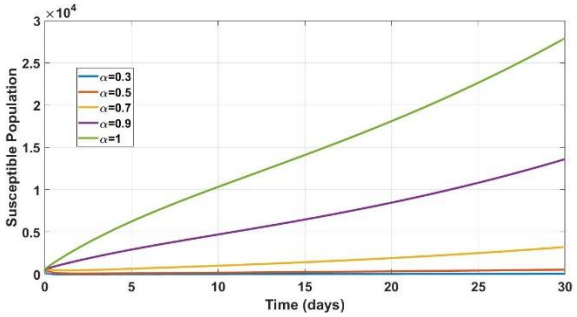

Figure 2

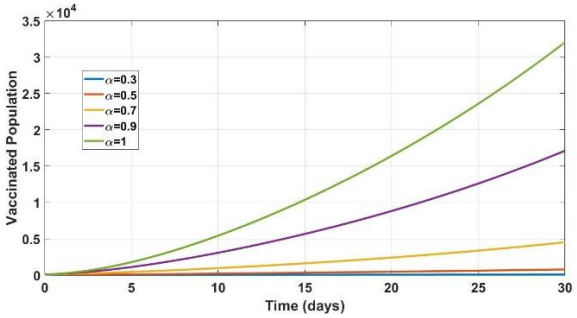

Figure 3

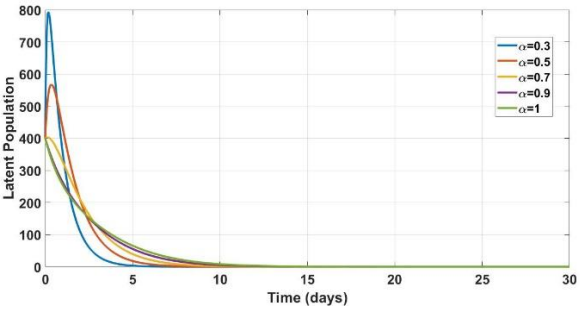

Figure 4

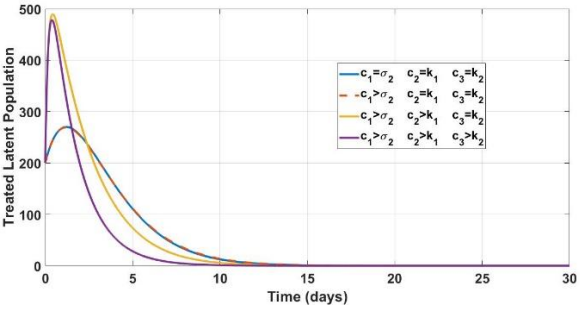

Figure 5

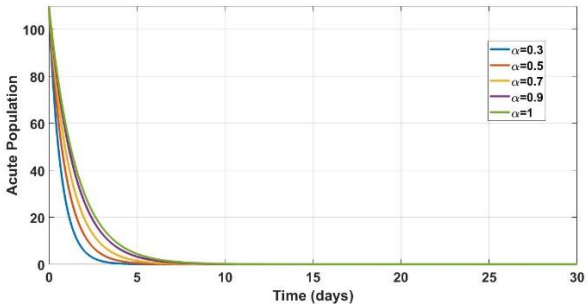

Figure 6

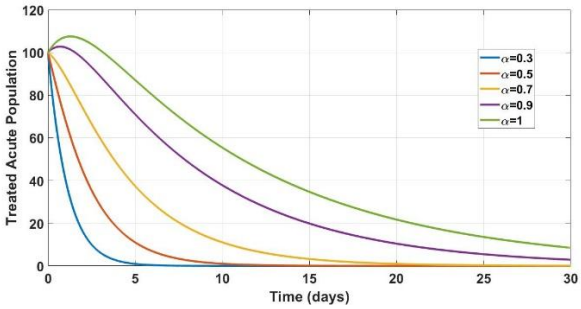

Figure 7

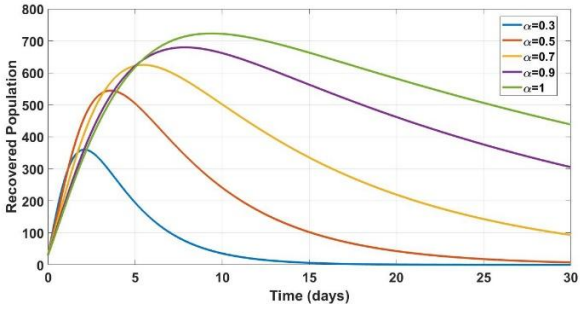

Figure 8

Figures 2 through 8 depict the dynamic models for each compartment, illustrating fractional variations.

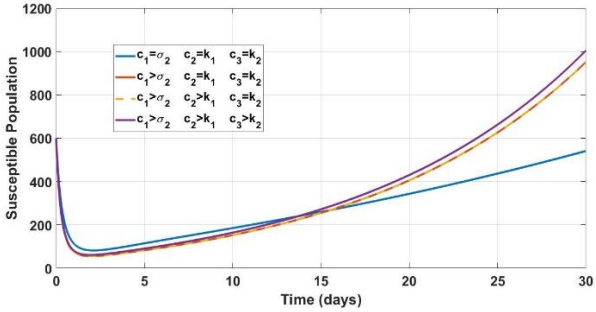

Figure 9

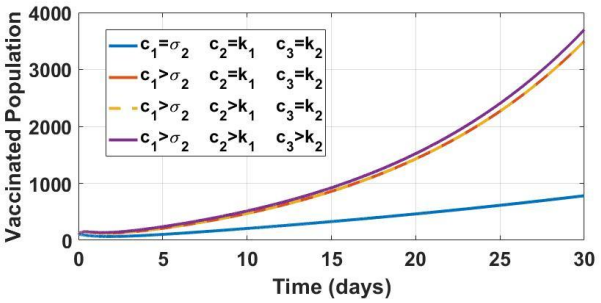

Figure 10

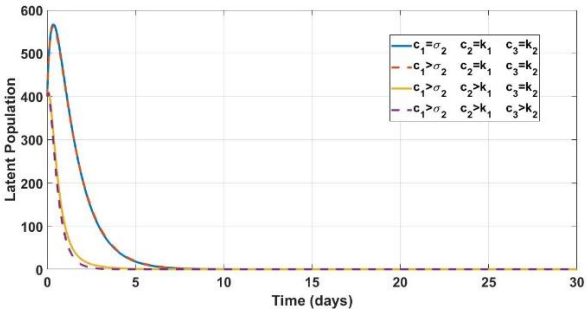

Figure 2

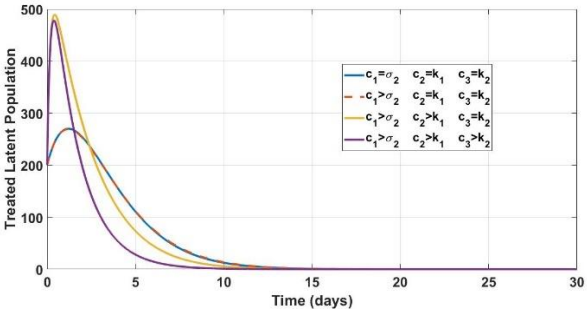

Figure 3

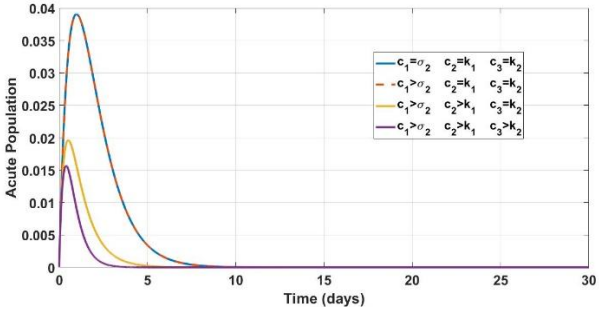

Figure 4

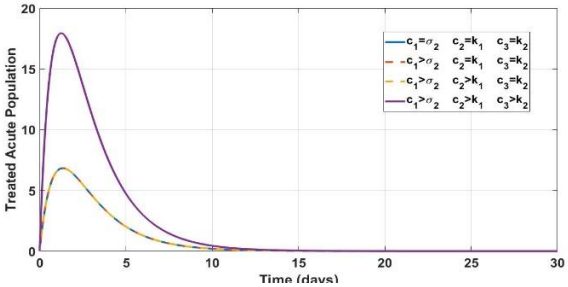

Figure 14

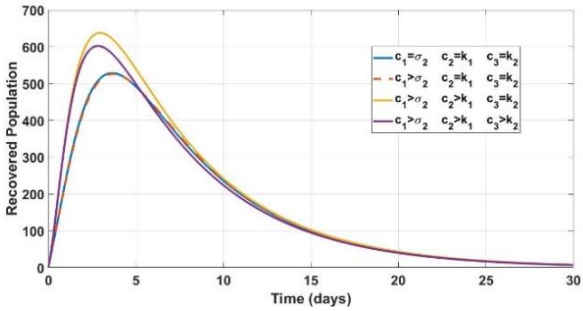

Figure 15

Figures 9 up to 15 illustrate the impact of optimal control on individual compartments.

Discussion of findings

Figures 2 through 8 provide a comprehensive graphical representation of the dynamic intricacies inherent in Fractional Ordinary Derivative Equations (FODEs) of equation 1, showcasing their numerical efficacy to describe biological systems when compared to conventional integer-order models. Significantly, the depicted solutions of the model, governed by the continuous evolution of the time-fractional derivative, consistently demonstrate convergence towards equilibrium points.

Figure 9 highlights the effects of these control measures on the susceptible population over time. With the initial implementation of control measures, there is a notable reduction in the susceptible population within the first 15 days. This decline is indicative of the effectiveness of the interventions in limiting the pool of individuals vulnerable to infection. However, beyond the 15-day mark, there is a subsequent increase in the susceptible population. This resurgence may be attributed to various factors, including waning immunity, incomplete vaccination coverage, or the emergence of new infectious strains. The depicted trend in Figure 10 illustrates that as the intensity of control measures escalates, particularly in terms of increasing vaccination coverage, there is a corresponding rise in the proportion of the population that has been vaccinated.

This suggests a positive correlation between the implementation of control strategies and the enhancement of population immunity, which is pivotal in mitigating disease transmission and potentially reducing the overall burden of illness within the community. As the control

measures are implemented and intensified, Figure 11 illustrates a notable reduction in the size of the latent population. This decline suggests that the combined efforts of vaccination, treatment of latent cases, and treatment of active infections effectively hinder the progression of the disease within the population. Such findings underscore the importance of multifaceted control strategies in mitigating the impact of infectious diseases and curtailing their spread. Figure 12 reveals a notable trend regarding the impact of these control measures on the treated latent population over time. Initially, as the control measures are implemented, there is a discernible increase in the latent treatment population observed within the first three days.

This suggests that the interventions are effective in identifying and treating individuals in the latent phase of infection promptly. However, beyond this initial period, the treated latent population shows a decrease, particularly noticeable from the fourth day onward. This decrease could indicate several potential dynamics within the disease system. It may imply a waning efficacy of the implemented control measures over time, highlighting the importance of sustained efforts in disease management. Alternatively, it could suggest a shift in the distribution of infected individuals within the population, necessitating adjustments in the allocation of resources and interventions to effectively target emerging hotspots of transmission. As the control measures are implemented and intensified,

Figure 13 illustrates a notable decrease in the population of actively infected individuals, denoted as the acute population. This reduction signifies the effectiveness of the implemented interventions in containing the spread of the disease and reducing the burden of acute cases within the population. These findings underscore the importance of targeted interventions in mitigating the impact of infectious diseases and highlight the potential of strategic control measures in epidemic management.

As depicted in Figure 14, an increase in control measure c3, corresponding to heightened efforts in treating actively infected individuals, leads to a notable rise in the population of treated acute cases. This trend suggests that allocating resources towards the treatment of actively infected individuals yields a discernible effect in managing the acute phase of the disease. Such findings underscore the importance of targeted treatment strategies in effectively controlling disease transmission and mitigating its impact on public health.

Figure 15 illustrates that the implementation of c1 and c2 results in notable increases in the proportion of the population that has recovered from the disease. This suggests that both individual vaccination and treatment of latent cases contribute positively to overall recovery rates. However, upon closer examination, it becomes apparent that the impact of c3, focused on treating active cases, is comparatively less effective in bolstering the recovered population. Despite its efforts, the increase in recovered individuals attributed to c3 is overshadowed by the substantial gains achieved through c1 and c2. This observation underscores the differential effectiveness of various control measures in shaping the trajectory of disease dynamics. While individual vaccination and treatment of latent cases exhibit significant promise in enhancing population-level recovery, the impact of treating active cases appears to be somewhat limited in comparison. Consequently, strategic allocation of resources and prioritization of interventions may be warranted to maximize the efficacy of disease control efforts and mitigate transmission within the population.

Conclusion

The results of this investigation underscore the multifaceted nature of control measures in influencing how infectious diseases spread within a population. Through comprehensive analysis of various interventions, including vaccination, and treatment of latent and active cases, results from simulations illuminate the differential impacts of these strategies on TB disease progression, population immunity, and recovery rates. While individual vaccination and treatment of latent cases demonstrate substantial efficacy in curbing transmission and enhancing recovery, the effectiveness of treating active cases appears comparatively limited. These insights emphasize the importance of strategic resource allocation and intervention prioritization to maximize the effectiveness of disease control efforts. By leveraging a combination of targeted measures, public health authorities can mitigate transmission, reduce disease burden, and safeguard population health against emerging threats.

Acknowledgement

Mrs Adetoun Loyinmi, and Sunday Oluwafemi Gbodogbe, are appreciated for their support.

REFERENCE

[1] World Health Organization Weekly Report, 2021. Available from: https://www.who.int/publications/i/item/9789240013131

[2] Ministry of Health, 2021. Available from: https://hsgm.saglik.gov.tr/tr/tuberkuloz-haberler/24-mart-dunya-tuberkuloz-gunu- etkinlikleri.html

[3] Tuberculosis Model, a Case Study of Tigania West, Kenya. Available online: https://www.researchgate.net/publication/308631904 (accessed on 2 January 2023).

[4] Tuberculosis Regional Factsheet. Available online:https://files.aho.afro.who.int/afahobckpcontainer/production/files/iAHO_TB_regional_Factsheet.pdf (accessed on 2 January 2023).

[5] Porous Border Blamed for TB Cases in Kenya and Ethiopia. Available online: https://www.theeastafrican.co.ke/tea/science-health/porous-border-blamed-for-tb-cases-in-kenya-and ethiopia-3764090 (accessed on 2 January 2023).

[6] Tuberculosis in Kenya. Available online: https://www.tbonline.info/media/uploads/documents/guidelines-on-management-of-leprosy--and-tuberculosis-in-kenya-(accessed on 2 January 2023).

[7] D. Young, J. Stark, D. Kirschner, "Systems Biology of Persistent Infection: Tuberculosis as a Case Study," *Nat. Rev. Microbiol.,* 6 (2008), 520–528. https://doi.org/10.1038/nrmicro1919

[8] K. O. Idowu, and A. C. Loyinmi, "Impact of Contaminated surfaces on the transmission dynamics of Corona Virus Disease (Covid-19)," *Biomedical Journal of Scientific and Technical Research,* 51, no. 1(2023), 42280–42294. https://doi.org/10.26717/BJSTR.2023.51.008046

[9] A. C. Loyinmi, and S. O. Gbodogbe, "Epidemiological viability and conrol of Rotavirus: A mathematical modelling approach," *FNAS Journal of Scientific Innovations*, 6, no. 2, (2025): 18-43.

[10] J. Gichuki, and D. Mategula, "Characterization of tuberculosis mortality in informal settlements in Nairobi,'' Kenya: Analysis of data between 2002 and 2016. BMC Infect. Dis. 2021, 21, 718.

[11] A. C. Loyinmi, S.O. Gbodogbe, and K.O. Idowu, "On the interaction of the human immune system with foreign body: mathematical modelling approach," *Kathmandu University Journal of Science, Engineering and Technology.* 17, no. 2 (2023): 1-17. https://journals.ku.edu.np/kuset/ article/view/137

[12] M. Yavuz, F., Özköse, M., Akman, and Z.T. Tastan, "A new mathematical model for tuberculosis epidemic under the consciousness effect," *Mathematical Modelling and Control*, 3, no.2 (2023); 88-103.

[13] J. O. Agbomola, and A. C. Loyinmi, "Modelling the impact of some control strategies on the transmission dynamics of Ebola virus in human-bat population: An optimal control analysis, "*Heliyon*, 8(12), e12121. 2022. https://doi.org/10.1016/j.heliyon.2022.e12121

[14] A. C. Loyinmi, T. K. Akinfe, and A. A. Ojo, "Qualitative analysis and dynamical behavior of a Lassa haemorrhagic fever model with exposed rodents and saturated incidence rate," *Scientific African*, 14, e01028. 2021. https://doi.org/10.1016/j.sciaf.2021.e01028

[15] A. C. Loyinmi, A. L. Ijaola, M. S. Shittu, and A. S.Ajala, "Qualitative and Mathematical analysis of COVID-19 with relapse and reinfection rate: A deterministic modelling approach," *FNAS Journal of Mathematical Modeling and Numerical Simulation*, 2, no.2 (2025), 118-131.

[16] O. K. Idowu, and A. C. Loyinmi, "Qualitative analysis of the transmission dynamics and optimal control of Covid-19," *EDUCATUM Journal of Science, Mathematics and Technology*. 10, no.1 (2023): 54–70. https://doi.org/10.37134/ejsmt.vol10.1.7.2023

[17] G. Gakii, and D. Malonza, "Mathematical Modeling of TB-HIV Co Infection, Case Study of Tigania West Sub County, Kenya," *J. Adv. Math. Comput. Sci*., 27 (2018): 1–18.

[18] N. P. Mnyambwa, D. Philbert, G. Kimaro, S. Wandiga, B. Kirenga, B.T. Mmbaga, and E. Ngadaya, "Gaps related to screening and diagnosis of tuberculosis in care cascade in selected health facilities in East Africa. countries: A retrospective study," *J. Clin. Tuberc. Other Mycobact*. Dis. 25 (2021): 100278.

[19] S. O. Gbodogbe, "Harmonizing epidemic dynamics: A fractional calculus approach to optimal control strategies for cholera transmission," *Scientific African*, 27 (2025): https://doi.org/10.1016/j.sciaf.2025.e02545

[20] A. C. Loyinmi, A. S. Ajala, and L. I. Alani, "Analysis of the effect of vaccination, efficient surveillance and treatment on the transmission dynamics of cholera," *Al-Bahir journal for Engineering and Pure Sciences*, 5, no. 2 (2024): 94–107. https://doi.org/10.55810/2313-0083.1070

[21] A. C. Loyinmi, and S. O. Gbodogbe, "Mathematical modeling and control strategies for Nipah virus transmission incorporating Bat – to – pig – to – human pathway,'' *EDUCATUM Journal of Science, Mathematics and Technology*, 11, no. 1 (2024): 54-80. https://doi.org/10.37134/ejsmt.vol11.1.7.2024

[22] K. A. Molla, M. A. Reta, and Y. Y. Ayene, "Prevalence of multi drug-resistant tuberculosis in East Africa: A systematic review and meta-analysis," *PLoS ONE*, 17 (2022): e0270272.

[23] K. Oshinubi, O. J. Peter, E. Addai, E. Mwizerwa, O. Babasola, I. V. Nwabufo, and J. O. Agbaje, "Mathematical modelling of tuberculosis outbreak in an East African country incorporating vaccination and treatment," *Computation*, 11, 7 (2023), 143. https://www.mdpi.com/2079-3197/11/7/143

[24] Kumama Regassa Cheneke, "Caputo Fractional Derivative for Analysis of COVID-19 and HIV/AIDS Transmission", Abstract and Applied Analysis, vol. 2023, Article ID 6371148, 12 pages, 2023. https://doi.org/10.1155/2023/6371148

[25] K. Logeswari, C. Ravichandran, and K. S. Nisar, "Mathematical model for spreading of COVID-19 virus with the Mittag–Leffler kernel," *Numerical Methods for Partial Differential Equations*, 40, no.1 (2024): e22652.

[26] A. C. Loyinmi, and A. L. Ijaola, "Investigating the effects of some controls measures on the dynamics of diphtheria infection using fractional order model," *Mathematics and Computational. Sciences*, 5, no. 4 (2024): 26-47 Doi:10.30511/MCS.2024.2032110.1183

[27] C. Loyinmi, and A. L. Ijaola, "Fractional order model of dynamical s and qualitative analysis of Anthrax with infected vector and saturation. *Int. J of Math. Anal. and Modelling,* 7, no.2 (2024): 224-264.

[28] S. Ahmad, A. Ullah, Q. M. Al-Mdallal, H. Khan, K. Shah, and A. Khan, "Fractional order Mathematical modeling of COVID-19 transmission," *Chaos, Solitons & Fractals*, 139, (2020); 110256.

[29] I. Podlubny, A. Chechkin, T. Skovranek, Y. Chen, B. M. V. Jara, 'Matrix approach to discrete fractional calculus II: Partial fractional differential equations,' *Journal of Computational Physics*, 228, no.8 (2009): 3137-3153.